Turkish Journal of Electrical Engineering & Computer Sciences

http://journals.tubitak.gov.tr/elektrik/

Research Article

Turk J Elec Eng & Comp Sci
(2015) 23: 1294 – 1311

doi:10.3906/elk-1306-163

Exact solution of conducting half plane problems in terms of a rapidly convergent series and an application of the multiplicative calculus

Ali UZER*
Department of Electrical and Electronics Engineering, Fatih University, İstanbul, Turkey

Received: 18.06.2013 • **Accepted/Published Online:** 05.08.2013 • **Printed:** 28.08.2015

Abstract: The problem of cylindrical wave incidence on a conducting half plane has been considered. A modal solution for Green's function of the problem is transformed into contour integral representations in a complex plane. Some contour deformations and changes of variables are then made for the integrals. Finally, the resultant integrals are transformed back into a series, which converges rapidly to the exact solution when the observation angles are close to the reflection/shadow boundaries (RSBs) of the conducting half plane. The multiplicative calculus is employed in deriving an expression that can be used for obtaining approximate solutions when the observation angles are away from the RSBs of the conducting half plane. The derived expressions are seen to be very simple for implementing in any computational environment.

Key words: Diffraction, conducting half plane, half plane screen, Sommerfeld problem, steepest descent method, multiplicative calculus

1. Introduction

The wave behavior near the edge of a conducting half plane has many important consequences in high frequency electromagnetics and acoustics. This famous problem has been considered for about a century by many authors. An exact solution for the plane wave incidence case was first given in [1]. The given solution involved Fresnel integrals, which can be evaluated by using the expressions given in mathematical handbooks such as [2].

A more general problem of cylindrical wave incidence on a conducting wedge was considered in [3], where its solution was given as contour integrals after transforming the modal solution of the problem into some integral representations. Later on, various asymptotic expansions were obtained from the integral representations by many authors. Specifically, an edge diffraction coefficient (called so in the terminology of the geometrical theory of diffraction (GTD)) was developed using asymptotically leading terms of those integral representations and then making some postulations as given in [4] in 1962. The authors of [5,6] applied a more advanced technique for the asymptotic evaluations of integrals and derived a more accurate expression for the edge diffraction coefficient in accordance with a method called the uniform theory of diffraction (UTD). The edge diffraction coefficient of UTD again involved Fresnel integrals, which have their own computational complexities.

The full details of the computational schemes of GTD and UTD for evaluations of the fields around a conducting half plane are provided in Section 2 and the computational complexities in those methods are demonstrated. After that we start from the modal solution of the conducting half plane problem and derive a new series whose terms involve only elementary functions (sine, cosine, and exponential functions). The newly

*Correspondence: aliuzer1@gmail.com

derived series has an interesting property of rapidly converging to the exact solution of the problem when the observation angles are close to the reflection/shadow boundaries (RSBs) of the conducting half plane. We could not detect a similar series for the exact solution of the problem in the literature.

In Section 3, we will also consider the complimentary case where the observation angles are away from the RSBs. We employ the multiplicative calculus [7] to derive an approximate expression that may be used whenever the series obtained in the first part of this paper is not rapidly convergent, i.e. when the observation angles are away from the RSBs.

The numerical results are given in Section 4, wherein the fields calculated by employing our expressions developed in Section 2 and Section 3 are compared with those calculated by using the schemes of GTD and UTD. The numerical results show that the fields calculated by using our expressions are more accurate than those calculated by the GTD or UTD methods.

2. Formulations for an exact solution

The electromagnetic waves around the edge of a conducting half plane can be determined by Green's function of the problem. There are two cases for Green's function. The first one is the hard polarization case, wherein the boundary condition is such that the derivative of Green's function with respect to the surface normal should be equal to zero on the surface of the conducting body. This type of boundary condition is also called the Neumann type boundary condition. The second one is the soft polarization case, wherein the boundary condition is such that Green's function itself should be equal to zero on the surface of the conducting body. This type of boundary condition is also called the Dirichlet type boundary condition. Green's function in the hard polarization case has been given as a modal solution [5] in the following form:

$$G_h(a,b,\phi,\phi') = g(a,b,\phi-\phi') + g(a,b,\phi+\phi'), \tag{1}$$

where

$$g(a,b,\beta) = \tfrac{1}{2}\sum_{m=0}^{\infty} \varepsilon_m J_{m/2}(ka) H^{(2)}_{m/2}(kb)\cos(m\beta/2), \tag{2}$$

$$\varepsilon_m = \begin{cases} 1 & , \quad m=0 \\ 2 & , \quad m \geq 1 \end{cases}, \tag{3}$$

where the subscript h means hard polarization, b and a denote respectively the distances of the source and observation points to the edge of the half plane, $\phi' and \phi$ denote respectively the angles of the source and observation points with respect to the half plane as shown in Figure 1, k is the wavenumber, $J_{m/2}(ka)$ denotes the Bessel function of the first kind, and $H^{(2)}_{m/2}(kb)$ denotes the Hankel function of the second kind. Green's function in the soft polarization case is equal to that obtained by negating the second term on the right-hand side in Eq. (1), i.e.:

$$G_s(a,b,\phi,\phi') = g(a,b,\phi-\phi') - g(a,b,\phi+\phi'), \tag{4}$$

where the subscript s means soft polarization.

The axial electric field due to an electric line source of strength I_e will be:

$$E_z = -\frac{\omega\mu}{4} I_e G_s(a,b,\phi,\phi'), \tag{5}$$

where μ denotes the permeability constant of the medium.

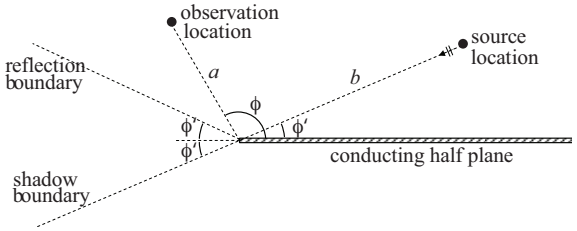

Figure 1. The conducting half plane problem. A line source at a point (b, ϕ') radiates a cylindrical wave and the field is observed at a point (a, ϕ). The reflection and shadow boundaries are called the RSBs of the problem. The high frequency methods have some difficulties for the field calculations near the RSBs.

The axial magnetic field due to a magnetic line source of strength I_m is expressible in terms of $G_h(a, b, \phi, \phi')$ as in:

$$H_z = \frac{\omega\varepsilon}{4} I_m G_h(a, b, \phi, \phi'), \tag{6}$$

where ε denotes the permittivity constant of the medium. Note that E_z in Eq. (5) satisfies the Dirichlet type boundary condition, whereas H_z in Eq. (6) satisfies the Neumann type boundary condition if the conducting plane is an electric conductor. If the conducting plane is a magnetic conductor, which is a theoretical concept and does not exist in nature, then Green's function in Eq. (5) should be replaced by $G_h(a, b, \phi, \phi')$ and that in Eq. (6) should be replaced by $G_s(a, b, \phi, \phi')$.

We need to focus on the evaluation of the function $g(a, b, \beta)$ since both hard and soft polarizations involve this function. Assuming $a < b$, the problem in the evaluation of this function is the slow convergence of the series when ka is large. Additionally, the Bessel functions need some computational labor. To avoid the slow convergence of the series and the intensive calculations of Bessel functions, GTD has developed a diffraction coefficient. The coefficient was developed essentially by transforming the series of Eq. (2) into a contour integral and then employing the steepest descent method [8]. According to GTD, the function $g(a, b, \beta)$ may be determined simply as a sum of two terms as in:

$$g(a, b, \beta) = H_0^{(2)}\left(k\sqrt{a^2 + b^2 - 2ab\cos\beta}\right) u(\pi - \beta) + \sqrt{\frac{2}{\pi kb}} e^{i\pi/4 - ikb} D(\beta) \frac{1}{\sqrt{a}} e^{-ika}, \tag{7}$$

where $D(\beta)$ is called the diffraction coefficient of the edge, which is given as follows:

$$D(\beta) = \frac{-e^{-i\pi/4}}{4\sqrt{2\pi k}} \left(\cot\tfrac{\pi+\beta}{4} + \cot\tfrac{\pi-\beta}{4}\right) = \frac{-e^{-i\pi/4}}{2\sqrt{2\pi k}\cos\frac{\beta}{2}}, \tag{8}$$

where $u(\pi - \beta)$ is the Heaviside unit step function that equals 1 when $\beta < \pi$, or equals 0 when $\beta > \pi$. The first term on the right-hand side in Eq. (7) is called an incident wave in the terminology of GTD, while the second term is called a diffracted wave. One limitation of the GTD is that the frequency (or the wavenumber k) and the distances (a and b) are postulated to be large. That means it is not possible to use Eq. (7) for determining the fields close to the edge of the half plane. Another limitation of the GTD is that the diffraction coefficient $D(\beta)$ in Eq. (8) loses accuracy as the RSB is approached (when $\cos\beta/2$ is small) and indeed it equals infinity just at the RSB (when $\cos\beta/2 = 0$). This deficiency has been solved by the UTD, wherein the

diffraction coefficient $D(\beta)$ is given as:

$$D(\beta) = \frac{-e^{-i\pi/4}}{2\sqrt{2\pi k}\cos\frac{\beta}{2}} F\left(2kL\cos^2\frac{\beta}{2}\right), \tag{9}$$

where $L = ab/(a+b)$, and $F(X)$ is called the transition function that is given in terms of a Fresnel integral:

$$F(X) = 2i\left|\sqrt{X}\right| e^{iX} \int_{|\sqrt{X}|}^{\infty} e^{-i\tau^2} d\tau. \tag{10}$$

This integral, in turn, has its own computational burden. Namely, approximations for this function are given as follows:

$$F(X) \cong \begin{cases} \left(\left|\sqrt{\pi X}\right| - 2Xe^{i\pi/4} - \frac{2}{3}X^2 e^{-i\pi/4}\right) e^{i(\pi/4+X)} & , \quad X < 0.3 \\ 1 + i\frac{1}{2X} - \frac{3}{4X^2} - i\frac{15}{8X^3} + \frac{75}{16X^4} & , \quad X > 5.5 \end{cases}, \tag{11}$$

whereas for intermediate values of the argument, $0.3 \leq X \leq 5.5$, [9] suggests making linear interpolations by using the data given in the Table. The implementation of this computational scheme for the calculation of $D(\beta)$ in Eq. (7) will be somewhat lengthy. Besides, the expression for the function $g(a,b,\beta)$ in Eq. (7) is itself an approximation for the original function given in Eq. (2), so even exact calculations of $F(X)$ do not yield an exact solution for the overall problem. Only for a plane wave incidence case does the expression of Eq. (7) become an exact representation, and then exact calculations of $F(X)$ will correspond to the exact solution for the overall problem.

Table. The values of the transition function $F(X)$ for linear interpolations as recommended by [9].

X	$F(X)$
0.3	0.5729+0.2677i
0.5	0.6768+0.2682i
0.7	0.7439+0.2549i
1.0	0.8095+0.2322i
1.5	0.8730+0.1982i
2.3	0.9240+0.1577i
4.0	0.9658+0.1073i
5.5	0.9797+0.0828i

Now we propose a completely different approach for the calculation of the original function $g(a,b,\beta)$ given in Eq. (2). It is possible to partition the series in Eq. (2) into two parts, one being on the even values of the summation index m and the other being on the odd values of m, as in:

$$g(a,b,\beta) = \tfrac{1}{2}\sum_{m=0}^{\infty} \varepsilon_{2m} J_m(ka) H_m^{(2)}(kb)\cos(m\beta) + \sum_{m=0}^{\infty} J_{\frac{2m+1}{2}}(ka) H_{\frac{2m+1}{2}}^{(2)}(kb)\cos\left(\tfrac{2m+1}{2}\beta\right), \tag{12}$$

where the first summation on the right-hand side can be evaluated exactly upon utilizing the addition theorem for Hankel functions [2], which can be expressed as:

$$\tfrac{1}{2}\sum_{m=0}^{\infty} \varepsilon_{2m} J_m(ka) H_m^{(2)}(kb)\cos(m\beta) = \tfrac{1}{2} H_0^{(2)}\left(k\sqrt{a^2+b^2-2ab\cos\beta}\right). \tag{13}$$

By using this property, the function $g(a,b,\beta)$ becomes:

$$g(a,b,\beta) = \tfrac{1}{2}H_0^{(2)}\left(k\sqrt{a^2+b^2-2ab\cos\beta}\right) + \sum_{m=0}^{\infty} J_{\frac{2m+1}{2}}(ka)H^{(2)}_{\frac{2m+1}{2}}(kb)\cos\left(\tfrac{2m+1}{2}\beta\right). \tag{14}$$

The product of the Bessel functions can be replaced by a contour integral representation given by [3]:

$$J_{m+1/2}(ka)H_{m+1/2}(kb) = -\frac{1}{2\pi}\int_C H_0^{(2)}\left(k\sqrt{a^2+b^2-2ab\cos\tau}\right)e^{i(m+1/2)\tau}d\tau, \tag{15}$$

where C denotes a contour in a complex τ plane as shown in Figure 2, where the path starts at $3\pi/2+i\infty$ and ends at $-\pi/2+i\infty$. If we substitute Eq. (15) into the series in Eq. (14), we obtain two geometric series under the integral operator as follows:

$$\begin{aligned}
&\sum_{m=0}^{\infty} J_{m+1/2}(ka)H^{(2)}_{m+1/2}(kb)\cos\left[(m+1/2)\,\beta\right] \\
&\quad = -\frac{1}{2\pi}\sum_{m=0}^{\infty}\int_C H_0^{(2)}\left(k\sqrt{a^2+b^2-2ab\cos\tau}\right)e^{i(m+1/2)\tau}\cos\left[(m+1/2)\beta\right]d\tau \\
&\quad = -\frac{1}{4\pi}\int_C H_0^{(2)}\left(k\sqrt{a^2+b^2-2ab\cos\tau}\right)\left(\sum_{m=0}^{\infty}e^{i(m+1/2)(\tau+\beta)}+\sum_{m=0}^{\infty}e^{i(m+1/2)(\tau-\beta)}\right)d\tau.
\end{aligned} \tag{16}$$

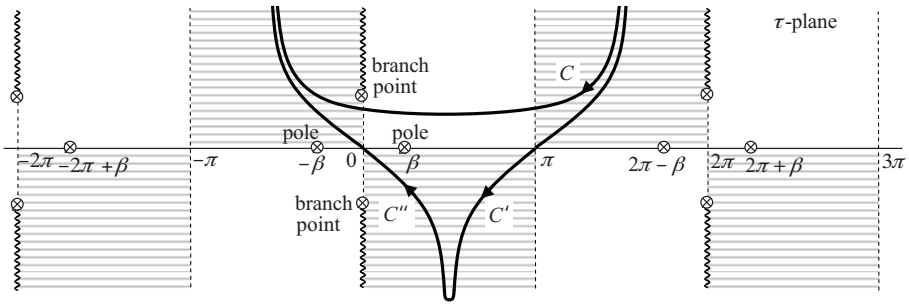

Figure 2. The poles and branch points of the integrand and the contours C, C', and C'' in the complex τ plane. Assume the contours C' and C'' are joined together at point $\pi/2-i\infty$ at infinity. The magnitude of the integrand in the shaded regions is smaller when compared with the magnitudes in the unshaded regions.

We employ the usual geometric series summation formula for the evaluation of the infinite summations in Eq. (16). For that, the absolute values of the term $e^{i(m+1/2)(\tau\pm\beta)}$ must be less than one, or equivalently the real part of $i\tau$ must be less than zero. This condition holds on the contour C since it lies on the upper half plane. We can do the following evaluations:

$$\begin{aligned}
&\sum_{m=0}^{\infty} e^{i(m+1/2)(\tau+\beta)} + \sum_{m=0}^{\infty} e^{i(m+1/2)(\tau-\beta)} \\
&\quad = e^{i(\tau+\beta)/2}\left[1+e^{i(\tau+\beta)}+e^{2i(\tau+\beta)}+\ldots\right] + e^{i(\tau-\beta)/2}\left[1+e^{i(\tau-\beta)}+e^{2i(\tau-\beta)}+\ldots\right] \\
&\quad = \frac{e^{i(\tau+\beta)/2}}{1-e^{i(\tau+\beta)}} + \frac{e^{i(\tau-\beta)/2}}{1-e^{i(\tau-\beta)}} = \frac{i\cos\frac{\beta}{2}\sin\frac{\tau}{2}}{\cos^2\frac{\beta}{2}-\cos^2\frac{\tau}{2}}.
\end{aligned} \tag{17}$$

Then, by substituting Eqs. (16) and (17) into Eq. (14), we get:

$$\begin{aligned} g(a,b,\beta) &= \tfrac{1}{2}H_0^{(2)}\left(k\sqrt{a^2+b^2-2ab\cos\beta}\right) \\ &\quad +\frac{1}{4\pi i}\int\limits_C H_0^{(2)}\left(k\sqrt{a^2+b^2-2ab\cos\tau}\right)\frac{\cos\frac{\beta}{2}\sin\frac{\tau}{2}}{\cos^2\frac{\beta}{2}-\cos^2\frac{\tau}{2}}d\tau, \end{aligned} \tag{18}$$

or we can simply write:

$$g(a,b,\beta)=\tfrac{1}{2}f(\beta)+\tfrac{1}{4\pi i}\int\limits_C \frac{f(\tau)\cos\frac{\beta}{2}\sin\frac{\tau}{2}}{\cos^2\frac{\beta}{2}-\cos^2\frac{\tau}{2}}d\tau, \tag{19}$$

where

$$f(\tau)=H_0^{(2)}\left(k\sqrt{a^2+b^2-2ab\cos\tau}\right). \tag{20}$$

The singularities of the integrand will be somewhat as shown in Figure 2. The poles will be at the points satisfying the equation $\cos^2\beta/2=\cos^2\tau/2$, which are:

$$\tau=\pm\beta+2\pi l; l=0,\pm1,\pm2,... \tag{21}$$

The branch points due to the square root function in the argument of the Hankel function in $f(\tau)$ will be at the points satisfying the equation $a^2+b^2-2ab\cos\tau=0$, which are:

$$\tau=\pm i\log\frac{a}{b}+2\pi l; l=0,\pm1,\pm2,... \tag{22}$$

Subsequently, we deform the contour C to $C'\cup C''$ as seen in Figure 2 where C' is passing through the point $\tau=\pi$, and C'' is passing through the origin $\tau=0$. One of the poles at $\tau=\beta$ or $\tau=2\pi-\beta$ will be swept during the deformation and this sweeping can be accounted as $2\pi i$ times the residue of the integrand in accordance with the Cauchy integral theorem. There are three possibilities: if $\beta<\pi$, then the pole at $\tau=\beta$ will lie in the interval $(0,\pi)$ and the residue contribution will be:

$$2\pi i\lim_{\tau\to\beta}\left\{\frac{\tau-\beta}{4\pi i}\frac{f(\tau)\cos\frac{\beta}{2}\sin\frac{\tau}{2}}{\cos^2\frac{\beta}{2}-\cos^2\frac{\tau}{2}}\right\}=\tfrac{1}{2}f(\beta)\cos\tfrac{\beta}{2}\sin\tfrac{\beta}{2}\lim_{\tau\to\beta}\frac{1}{\frac{1}{2}2\cos\frac{\tau}{2}\sin\frac{\tau}{2}}=\tfrac{1}{2}f(\beta); \tag{23}$$

if $\beta>\pi$, then the pole at $\tau=2\pi-\beta$ will lie in the interval $(0,\pi)$ and so the residue should be evaluated with respect to this pole as follows:

$$2\pi i\lim_{\tau\to2\pi-\beta}\left\{\frac{\tau-2\pi+\beta}{4\pi i}\frac{f(\tau)\cos\frac{\beta}{2}\sin\frac{\tau}{2}}{\cos^2\frac{\beta}{2}-\cos^2\frac{\tau}{2}}\right\}=\lim_{\tau\to2\pi-\beta}\frac{\frac{1}{2}f(\beta)\cos\frac{\beta}{2}\sin\frac{2\pi-\beta}{2}}{\frac{1}{2}2\cos\frac{\tau}{2}\sin\frac{\tau}{2}}=-\tfrac{1}{2}f(\beta); \tag{24}$$

if $\beta=\pi$, then the poles at $\tau=\beta$ and $\tau=2\pi-\beta$ coincide and the integrand equals exactly zero. That means the residue contribution will be zero.

As we see, the sign of the answer depends on the magnitude of β. This sign variation is expressible in terms of the sign function sgn so that the residue contribution will be

$$\tfrac{1}{2}f(\beta)sgn\left(\cos\tfrac{\beta}{2}\right) \tag{25}$$

for any value of β. The function $g(a,b,\beta)$ after deforming C to $C' \cup C''$ will be

$$\begin{aligned} g(a,b,\beta) &= \tfrac{1}{2}f(\beta) + \tfrac{1}{2}f(\beta)sgn\left(\cos\tfrac{\beta}{2}\right) \\ &+ \frac{1}{4\pi i}\int\limits_{C'} \frac{f(\tau)\cos\frac{\beta}{2}\sin\frac{\tau}{2}}{\cos^2\frac{\beta}{2}-\cos^2\frac{\tau}{2}}d\tau + \frac{1}{4\pi i}\int\limits_{C''} \frac{f(\tau)\cos\frac{\beta}{2}\sin\frac{\tau}{2}}{\cos^2\frac{\beta}{2}-\cos^2\frac{\tau}{2}}d\tau. \end{aligned} \tag{26}$$

One can easily show that the integral along C'' must be exactly zero. This is so because the path of C'' is symmetric with respect to the origin on the τ plane, while the integrand is an odd function of τ; that is:

$$\frac{f(-\tau)\cos\frac{\beta}{2}\sin\frac{-\tau}{2}}{\cos^2\frac{\beta}{2}-\cos^2\frac{-\tau}{2}} = -\frac{f(\tau)\cos\frac{\beta}{2}\sin\frac{\tau}{2}}{\cos^2\frac{\beta}{2}-\cos^2\frac{\tau}{2}} \tag{27}$$

and

$$\begin{aligned} \frac{1}{4\pi i}\int\limits_{C''} \frac{f(\tau)\cos\frac{\beta}{2}\sin\frac{\tau}{2}}{\cos^2\frac{\beta}{2}-\cos^2\frac{\tau}{2}}d\tau &= \frac{1}{4\pi i}\int\limits_{\pi/2-i\infty}^{0} \frac{f(\tau)\cos\frac{\beta}{2}\sin\frac{\tau}{2}}{\cos^2\frac{\beta}{2}-\cos^2\frac{\tau}{2}}d\tau + \frac{1}{4\pi i}\int\limits_{0}^{-\pi/2+i\infty} \frac{f(\tau)\cos\frac{\beta}{2}\sin\frac{\tau}{2}}{\cos^2\frac{\beta}{2}-\cos^2\frac{\tau}{2}}d\tau \\ &= \frac{1}{4\pi i}\int\limits_{-\pi/2+i\infty}^{0} \frac{f(-\tau)\cos\frac{\beta}{2}\sin\frac{-\tau}{2}}{\cos^2\frac{\beta}{2}-\cos^2\frac{-\tau}{2}}(-d\tau) + \frac{1}{4\pi i}\int\limits_{0}^{-\pi/2+i\infty} \frac{f(\tau)\cos\frac{\beta}{2}\sin\frac{\tau}{2}}{\cos^2\frac{\beta}{2}-\cos^2\frac{\tau}{2}}d\tau \\ &= \frac{1}{4\pi i}\int\limits_{-\pi/2+i\infty}^{0} \frac{f(\tau)\cos\frac{\beta}{2}\sin\frac{\tau}{2}}{\cos^2\frac{\beta}{2}-\cos^2\frac{\tau}{2}}d\tau + \frac{1}{4\pi i}\int\limits_{0}^{-\pi/2+i\infty} \frac{f(\tau)\cos\frac{\beta}{2}\sin\frac{\tau}{2}}{\cos^2\frac{\beta}{2}-\cos^2\frac{\tau}{2}}d\tau. \end{aligned} \tag{28}$$

The function in Eq. (26) reduces to:

$$g(a,b,\beta) = \tfrac{1}{2}f(\beta) + \tfrac{1}{2}f(\beta)sgn\left(\cos\tfrac{\beta}{2}\right) + \tfrac{1}{4\pi i}\int\limits_{C'} \frac{f(\tau)\cos\frac{\beta}{2}\sin\frac{\tau}{2}}{\cos^2\frac{\beta}{2}-\cos^2\frac{\tau}{2}}d\tau. \tag{29}$$

For the integration along C', it is convenient to make a change of variable, $\tau = z + \pi$. Then the contour C' will be translated to C_z as shown in Figure 3 and Eq. (29) becomes:

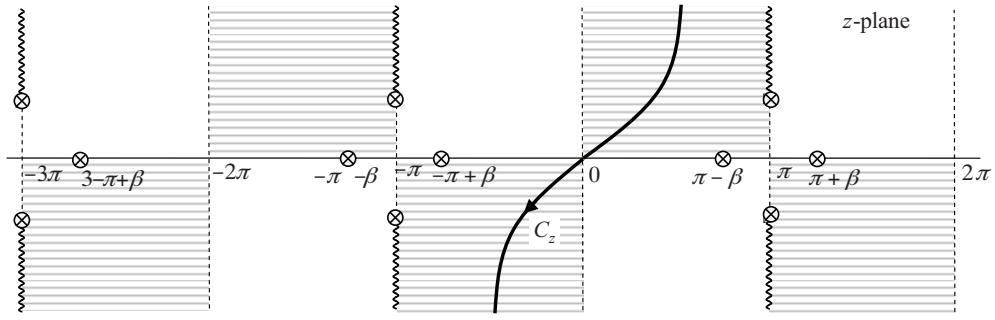

Figure 3. The contour C_z in the z plane, which is simply a translation of C' due to the change of variable $\tau = z + \pi$.

$$g(a,b,\beta) = \tfrac{1}{2}f(\beta) + \tfrac{1}{2}f(\beta)sgn\left(\cos\tfrac{\beta}{2}\right) + I(a,b,\beta), \tag{30}$$

where

$$I(a,b,\beta) = \frac{1}{4\pi i}\int\limits_{C_z} f(z+\pi)\frac{\cos\frac{\beta}{2}\sin\frac{z+\pi}{2}}{\sin^2\frac{z+\pi}{2} - \sin^2\frac{\beta}{2}}dz, \tag{31}$$

or, by using

$$\begin{aligned} &\sin^2\tfrac{z+\pi}{2} = 1 - \sin^2\tfrac{z}{2} \\ &1 - \sin^2\tfrac{\beta}{2} = \cos^2\tfrac{\beta}{2} \\ &f(z+\pi) = H_0^{(2)}\left(k\sqrt{a^2+b^2-2ab\cos(z+\pi)}\right) = H_0^{(2)}\left(k\sqrt{(a+b)^2-4ab\sin^2\tfrac{z}{2}}\right) \end{aligned} \tag{32}$$

we can write:

$$I(a,b,\beta) = \frac{1}{4\pi i}\int\limits_{C_z} H_0^{(2)}\left(k\sqrt{(a+b)^2-4ab\sin^2\tfrac{z}{2}}\right)\frac{\cos\frac{\beta}{2}\cos\frac{z}{2}}{\cos^2\frac{\beta}{2} - \sin^2\frac{z}{2}}dz. \tag{33}$$

Consider a change of variable:

$$\begin{aligned} \sin\tfrac{z}{2} &= \left|\cos\tfrac{\beta}{2}\right|\sin\tfrac{w}{2} \\ \cos\tfrac{z}{2}dz &= \left|\cos\tfrac{\beta}{2}\right|\cos\tfrac{w}{2}dw \end{aligned}. \tag{34}$$

The integral in Eq. (33) with the change of variable becomes:

$$\begin{aligned} I(a,b,\beta) &= \frac{1}{4\pi i}\int\limits_{C_w} H_0^{(2)}\left(k\sqrt{(a+b)^2-4ab\cos^2\tfrac{\beta}{2}\sin^2\tfrac{w}{2}}\right)\frac{\cos\frac{\beta}{2}\left|\cos\frac{\beta}{2}\right|\cos\frac{w}{2}}{\cos^2\frac{\beta}{2} - \cos^2\frac{\beta}{2}\sin^2\frac{w}{2}}dw \\ &= \frac{\mathrm{sgn}(\cos\frac{\beta}{2})}{4\pi i}\int\limits_{C_w} H_0^{(2)}\left(k\sqrt{(a+b)^2-4ab\cos^2\tfrac{\beta}{2}\sin^2\tfrac{w}{2}}\right)\frac{dw}{\cos\frac{w}{2}}. \end{aligned} \tag{35}$$

The contour C_w in the w plane will be somewhat as shown in Figure 4. C_w may be taken to be the image of the contour C_z under a mapping:

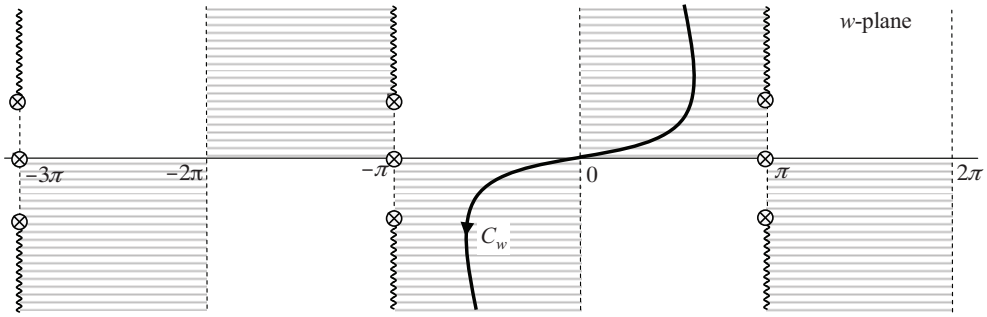

Figure 4. The contour C_w in the w plane, which is the image of the contour C_z under a mapping $w = 2\sin^{-1}\left(\sin\frac{z}{2}/\left|\cos\frac{\beta}{2}\right|\right)$, where C_z is shown in the previous figure.

$$w = 2\sin^{-1}\left(\sin\tfrac{z}{2}/\left|\cos\tfrac{\beta}{2}\right|\right). \tag{36}$$

It can be shown that the end points of C_w and C_z are the same, and so are their intersection points with the real axes as seen from Figures 3 and 4, because:

$$\begin{aligned} &2\sin^{-1}\left[\sin\left(\tfrac{\pi/2+i\infty}{2}\right)/\left|\cos\tfrac{\beta}{2}\right|\right] = \pi/2+i\infty \\ &2\sin^{-1}\left[\sin\left(\tfrac{0}{2}\right)/\left|\cos\tfrac{\beta}{2}\right|\right] = 0 \\ &2\sin^{-1}\left[\sin\left(\tfrac{-\pi/2-i\infty}{2}\right)/\left|\cos\tfrac{\beta}{2}\right|\right] = -\pi/2-i\infty \end{aligned}. \tag{37}$$

The poles of the integrand in Eq. (35) will be at the points satisfying the equation $\cos w/2 = 0$, which are:

$$w = \pm\pi + 2\pi l; l = 0, \pm1, \pm2, ..., \tag{38}$$

as shown in Figure 4. The branch points will be at the points satisfying the equation $(a+b)^2 - 4ab\cos^2\frac{\beta}{2}\sin^2\frac{w}{2} = 0$, which yields a solution:

$$w = \pm\pi \pm i\log\frac{a+b-\sqrt{a^2+b^2-2ab\cos\beta}}{a+b+\sqrt{a^2+b^2-2ab\cos\beta}} + 2\pi l; l = 0, \pm1, \pm2, ... \tag{39}$$

We proceed by writing an equation:

$$(a+b)^2 - 4ab\cos^2\tfrac{\beta}{2}\sin^2\tfrac{w}{2} = (p+q)^2 - 4pq\sin^2\tfrac{w}{2} \tag{40}$$

and solving it for p and q as follows. It holds if:

$$\begin{aligned} a+b &= p+q \\ ab\cos^2\tfrac{\beta}{2} &= pq \end{aligned}. \tag{41}$$

Therefore, the solution for p and q will be

$$\begin{aligned} p &= \tfrac{1}{2}\left(a+b-\sqrt{a^2+b^2-2ab\cos\beta}\right) \\ q &= \tfrac{1}{2}\left(a+b+\sqrt{a^2+b^2-2ab\cos\beta}\right) \end{aligned} \tag{42}$$

and Eq. (35) can be written as:

$$\begin{aligned} I(a,b,\beta) &= \frac{sgn\left(\cos\frac{\beta}{2}\right)}{4\pi i}\int\limits_{C_w} H_0^{(2)}\left(k\sqrt{(p+q)^2-4pq\sin^2\tfrac{w}{2}}\right)\frac{dw}{\cos\frac{w}{2}} \\ &= \frac{sgn\left(\cos\frac{\beta}{2}\right)}{4\pi i}\int\limits_{C_w} H_0^{(2)}\left(k\sqrt{p^2+q^2+2pq\cos w}\right)\frac{dw}{\cos\frac{w}{2}}. \end{aligned} \tag{43}$$

If we deform the contour C_w to $C'_w \cup C''_w$ as seen in Figure 5, we need to write:

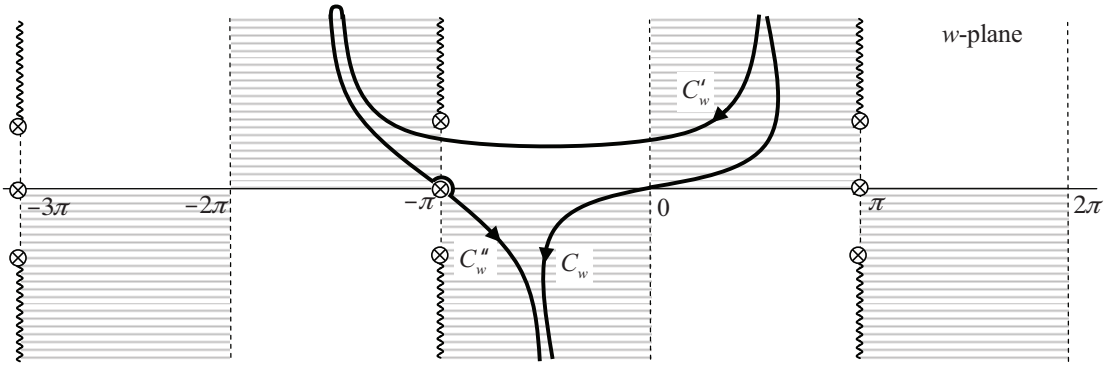

Figure 5. The contours C'_w and C''_w after the deformation of C_w in the w plane. The pole at $w=-\pi$ is encircled one-half times in the clockwise direction by the contour C''_w and this will amount to a residue contribution that is equal to $-\pi i$ times the residue of the integrand at $w=-\pi$ as calculated in Eq. (45). Assume the contours C'_w and C''_w are joined together at point $-3\pi/2+i\infty$ at infinity.

$$\begin{aligned} I(a,b,\beta) &= \frac{sgn\left(\cos\frac{\beta}{2}\right)}{4\pi i}\int\limits_{C'_w} H_0^{(2)}\left(k\sqrt{p^2+q^2+2pq\cos w}\right)\frac{dw}{\cos\frac{w}{2}} \\ &\quad + \frac{sgn\left(\cos\frac{\beta}{2}\right)}{4\pi i}\int\limits_{C''_w} H_0^{(2)}\left(k\sqrt{p^2+q^2+2pq\cos w}\right)\frac{dw}{\cos\frac{w}{2}}. \end{aligned} \tag{44}$$

Note that a pole at $w=-\pi$ is encircled $1/2$ times in the clockwise direction by the contour C''_w. Its contribution will be equal to $-\pi i$ times the residue of the integrand, according to the Cauchy integral theorem, which is:

$$\begin{aligned} &-\pi i \lim_{w\to-\pi}\left\{(w+\pi)\frac{sgn\left(\cos\frac{\beta}{2}\right)}{4\pi i}H_0^{(2)}\left(k\sqrt{p^2+q^2+2pq\cos w}\right)\frac{1}{\cos\frac{w}{2}}\right\} \\ &\quad = -\tfrac{1}{2}sgn\left(\cos\tfrac{\beta}{2}\right)H_0^{(2)}\left(k\sqrt{a^2+b^2-2ab\cos\beta}\right) = -\tfrac{1}{2}sgn\left(\cos\tfrac{\beta}{2}\right)f(\beta). \end{aligned} \tag{45}$$

Hence, $I(a,b,\beta)$ becomes:

$$\begin{aligned} I(a,b,\beta) &= -\tfrac{1}{2}sgn\left(\cos\tfrac{\beta}{2}\right)f(\beta) \\ &\quad + \frac{sgn\left(\cos\frac{\beta}{2}\right)}{4\pi i}\int\limits_{C'_w} H_0^{(2)}\left(k\sqrt{p^2+q^2+2pq\cos w}\right)\frac{dw}{\cos\frac{w}{2}}. \end{aligned} \tag{46}$$

Let us make a change of variable $w=\tau-\pi$ in this integral. Then C'_w becomes C in the τ plane (shown in

Figure 2), and $I(a,b,\beta)$ becomes:

$$\begin{aligned} I(a,b,\beta) &= -\tfrac{1}{2}sgn\left(\cos\tfrac{\beta}{2}\right)f(\beta)+\frac{sgn\left(\cos\frac{\beta}{2}\right)}{4\pi i}\int\limits_C H_0^{(2)}\left(k\sqrt{p^2+q^2+2pq\cos(\tau-\pi)}\right)\frac{d\tau}{\cos\frac{\tau-\pi}{2}} \\ &= -\tfrac{1}{2}sgn\left(\cos\tfrac{\beta}{2}\right)f(\beta)+\frac{sgn\left(\cos\frac{\beta}{2}\right)}{4\pi i}\int\limits_C H_0^{(2)}\left(k\sqrt{p^2+q^2+2pq\cos\tau}\right)\frac{d\tau}{\sin\frac{\tau}{2}}. \end{aligned} \tag{47}$$

After substituting Eq. (47) into Eq. (30), we get:

$$g(a,b,\beta)=\tfrac{1}{2}f(\beta)+\frac{sgn\left(\cos\frac{\beta}{2}\right)}{4\pi i}\int\limits_C H_0^{(2)}\left(k\sqrt{p^2+q^2-2pq\cos\tau}\right)\frac{d\tau}{\sin\frac{\tau}{2}}. \tag{48}$$

If we expand $1/\sin(\tau/2)$ into a series

$$\frac{1}{\sin\frac{\tau}{2}}=\frac{2i}{e^{i\tau/2}-e^{-i\tau/2}}=-2ie^{i\tau/2}\frac{1}{1-e^{i\tau}}=-2ie^{i\tau/2}\left(1+e^{i\tau}+e^{2i\tau}+...\right)=-2i\sum_{m=0}^{\infty}e^{i(2m+1)\tau/2} \tag{49}$$

because $\left|e^{i(2m+1)\tau/2}\right|<1 on\, C$, then $g(a,b,\beta)$ becomes:

$$\begin{aligned} g(a,b,\beta) &= \tfrac{1}{2}f(\beta)+\frac{sgn\left(\cos\frac{\beta}{2}\right)}{4\pi i}\int\limits_C H_0^{(2)}\left(k\sqrt{p^2+q^2-2pq\cos\tau}\right)\left(-2i\sum_{m=0}^{\infty}e^{i(2m+1)\tau/2}\right)d\tau \\ &= \tfrac{1}{2}f(\beta)-\frac{sgn\left(\cos\frac{\beta}{2}\right)}{2\pi}\sum_{m=0}^{\infty}\int\limits_C H_0^{(2)}\left(k\sqrt{p^2+q^2-2pq\cos\tau}\right)e^{i(m+1/2)\tau}d\tau. \end{aligned} \tag{50}$$

Now we can replace the integral by products of the Bessel functions by employing Eq. (15) in the reverse direction:

$$\int\limits_C H_0^{(2)}\left(k\sqrt{p^2+q^2-2pq\cos\tau}\right)e^{i(m+1/2)\tau}d\tau=-2\pi\sum_{m=0}^{\infty}J_{m+1/2}(kp)H_{m+1/2}(kq), \tag{51}$$

which leads to:

$$g(a,b,\beta)=\tfrac{1}{2}f(\beta)+sgn\left(\cos\tfrac{\beta}{2}\right)\sum_{m=0}^{\infty}J_{m+1/2}(kp)H_{m+1/2}(kq), \tag{52}$$

or, using Eq. (20) and Eq. (42):

$$\begin{aligned} g(a,b,\beta) &= \tfrac{1}{2}H_0^{(2)}\left(k\sqrt{a^2+b^2-2ab\cos\beta}\right)+sgn\left(\cos\tfrac{\beta}{2}\right) \\ &\cdot\sum_{m=0}^{\infty}J_{m+1/2}\left[\tfrac{k}{2}\left(a+b-\sqrt{a^2+b^2-2ab\cos\beta}\right)\right]H_{m+1/2}^{(2)}\left[\tfrac{k}{2}\left(a+b+\sqrt{a^2+b^2-2ab\cos\beta}\right)\right], \end{aligned} \tag{53}$$

which will be convenient for numerical computations when β is close to the RSB. The convergence of this series will speed up as the RSB is approached (when $\beta\to\pm\pi$). More interestingly, it is valid even if the distances to the edge (a, b, or both of them) are lowered. This behavior is in contrast to all high frequency methods wherein, as a postulation, those distances should be large in terms of the wavelength. Such a representation for

conducting half plane problems does not exist in the literature and it must be novel. Note that we have not made any approximation and $g(a,b,\beta)$ in Eq. (53) is still an exact representation.

The Bessel functions of half-integer order, as in Eq. (53), are expressible in terms of elementary functions as follows [2]:

$$\begin{aligned} J_{m+\frac{1}{2}}(z) &= \tfrac{\sqrt{2z}}{\sqrt{\pi}} z^m \left(-\tfrac{1}{z}D_z\right)^m \left\{\tfrac{\sin z}{z}\right\} \\ H^{(2)}_{m+\frac{1}{2}}(z) &= \tfrac{\sqrt{2z}}{\sqrt{\pi}} z^m \left(-\tfrac{1}{z}D_z\right)^m \left\{\tfrac{ie^{-iz}}{z}\right\} \end{aligned}, \tag{54}$$

where D_z means the differentiation operator with respect to z. A few of those functions, which we use in our numerical calculations, are as follows.

$$\begin{aligned} J_{0.5}(z) &= \tfrac{\sqrt{2z}}{z\sqrt{\pi}} \sin z \\ J_{1.5}(z) &= \tfrac{-\sqrt{2z}}{z^2\sqrt{\pi}} \left[z\cos z - \sin z\right] \\ J_{2.5}(z) &= \tfrac{-\sqrt{2z}}{z^3\sqrt{\pi}} \left[\left(z^2-3\right)\sin z + 3z\cos z\right] \\ J_{3.5}(z) &= \tfrac{\sqrt{2z}}{z^4\sqrt{\pi}} \left[\left(z^3-15z\right)\cos z - \left(6z^2-15\right)\sin z\right] \\ J_{4.5}(z) &= \tfrac{\sqrt{2z}}{z^5\sqrt{\pi}} \left[\left(z^4-45z^2+105\right)\sin z - \left(105z-10z^3\right)\cos z\right] \\ J_{5.5}(z) &= \tfrac{-\sqrt{2z}}{z^6\sqrt{\pi}} \left[\left(z^5-105z^3+945z\right)\cos z - \left(15z^4-420z^2+945\right)\sin z\right] \end{aligned} \tag{55}$$

$$\begin{aligned} H^{(2)}_{0.5}(z) &= \tfrac{i\sqrt{2z}e^{-iz}}{z\sqrt{\pi}} \\ H^{(2)}_{1.5}(z) &= \tfrac{i\sqrt{2z}e^{-iz}}{z^2\sqrt{\pi}} \left(1+iz\right) \\ H^{(2)}_{2.5}(z) &= \tfrac{i\sqrt{2z}e^{-iz}}{z^3\sqrt{\pi}} \left(-z^2+3iz+3\right) \\ H^{(2)}_{3.5}(z) &= \tfrac{i\sqrt{2z}e^{-iz}}{z^4\sqrt{\pi}} \left(-iz^3-6z^2+15iz+15\right) \\ H^{(2)}_{4.5}(z) &= \tfrac{i\sqrt{2z}e^{-iz}}{z^5\sqrt{\pi}} \left(z^4-10iz^3-45z^2+105iz+105\right) \\ H^{(2)}_{5.5}(z) &= \tfrac{i\sqrt{2z}e^{-iz}}{z^6\sqrt{\pi}} \left(iz^5+15z^4-105iz^3-420z^2+945iz+945\right) \end{aligned} \tag{56}$$

3. Formulations for an approximate solution

When β is not close to the RSB, the expression in Eq. (53) does not give an appreciable advantage. In such a case one may employ the conventional GTD or UTD techniques wherein $g(a,b,\beta)$ may be determined via Eq. (7) and the approximations given in Section 2. Alternatively, we can derive a more accurate expression by employing the steepest descent method to the integral in Eq. (43). To begin with, we need to replace the Hankel function by an asymptotically leading term:

$$H_0^{(2)}\left(k\sqrt{p^2+q^2+2pq\cos w}\right) \cong \sqrt{\frac{2i}{\pi k(p+q)}} \frac{e^{-ik(p+q)\sqrt{1-4M\sin^2 w/2}}}{\left(1-4M\sin^2\frac{w}{2}\right)^{1/4}};\ as\ p+q\to\infty, \tag{57}$$

where

$$M = \frac{pq}{(p+q)^2}, \tag{58}$$

and so $I(a,b,\beta)$ in Eq. (43) can be written as

$$I(a,b,\beta) \cong \frac{sgn\left(\cos\frac{\beta}{2}\right)}{4\pi i}\sqrt{\frac{2i}{\pi k(p+q)}}J(p,q,\beta), \tag{59}$$

where

$$J(p,q,\beta) = \int\limits_{C_w} \frac{e^{-ik(p+q)\sqrt{1-4M\sin^2\frac{w}{2}}}}{\left(1-4M\sin^2\frac{w}{2}\right)^{1/4}}\frac{dw}{\cos\frac{w}{2}} \tag{60}$$

is to be evaluated as $p+q\to\infty$ by using the steepest descent method [8]. Let us make a change of variable:

$$\begin{aligned} s &= e^{3i\pi/4}\sin\tfrac{w}{2} \\ ds &= e^{3i\pi/4}\tfrac{1}{2}\cos\tfrac{w}{2}dw \end{aligned}. \tag{61}$$

This will map the critical points (the end points and the origin) of the contour C_w onto the real axis since

$$\begin{aligned} e^{3i\pi/4}\sin\tfrac{\pi/2+i\infty}{2} &= -\infty \\ e^{3i\pi/4}\sin\tfrac{0}{2} &= 0 \\ e^{3i\pi/4}\sin\tfrac{-\pi/2-i\infty}{2} &= \infty \end{aligned} \tag{62}$$

so that $J(p,q,\beta)$ becomes an integral along the real axis:

$$J(p,q,\beta) \cong \int\limits_{-\infty}^{\infty} \frac{e^{-ik(p+q)\sqrt{1-4iMs^2}}}{(1-4iMs^2)^{1/4}}\frac{2e^{-3i\pi/4}ds}{1-is^2}. \tag{63}$$

Note that $s=0$ is a saddle point and, therefore, we need to expand the amplitude and phase terms into Taylor series. An alternative way for achieving a more accurate expansion, according to our experience, is to employ the multiplicative calculus [7] when making expansions for the functions. The Taylor "series" expansion in the classical calculus is analogous to a Taylor "product" expansion in the multiplicative calculus. In the sense of the multiplicative calculus, we can do the Taylor product expansions as follows:

$$\frac{1}{1-is^2} = e^{-\log(1-is^2)} = e^{is^2-s^4/2-is^6/3+O(s^8)}, \tag{64}$$

$$\begin{aligned} \frac{e^{-ik(p+q)\sqrt{1-4iMs^2}}}{(1-4iMs^2)^{1/4}} &= e^{-ik(p+q)\sqrt{1-4iMs^2}-\frac{1}{4}\log\left(1-4iMs^2\right)} \\ &= e^{-ik(p+q)-(2k(p+q)-i)Ms^2-2(ik(p+q)+1)M^2s^4-4(-k(p+q)+4i/3)M^3s^6+O(s^8)}, \end{aligned} \tag{65}$$

where O denotes the Landau symbol. Then $J(p,q,\beta)$ becomes

$$J(p,q,\beta) \cong 2e^{-3i\pi/4-ik(p+q)}\int\limits_{-\infty}^{\infty} e^{-c_2s^2-c_4s^4-c_6s^6+O(s^8)}ds, \tag{66}$$

where the coefficients are:

$$\begin{aligned} c_2 &= (2k(p+q)-i)\,\tfrac{pq}{(p+q)^2} - i \\ c_4 &= 2\,(ik(p+q)+1)\,\tfrac{p^2q^2}{(p+q)^4} + \tfrac{1}{2} \\ c_6 &= 4\left(-k(p+q)+\tfrac{4i}{3}\right)\tfrac{p^3q^3}{(p+q)^6} + \tfrac{i}{3} \end{aligned} \quad . \tag{67}$$

It can be shown that

$$e^{-c_2s^2-c_4s^4-c_6s^6+O(s^8)} = e^{-c_2s^2} - c_4s^4e^{-(c_2-c_6/c_4)s^2} + O(s^8). \tag{68}$$

The proof can be given simply by expanding both sides of the equation into power series in s and then collecting the same powers of s. By substituting Eq. (68) into Eq. (66), we obtain:

$$J(p,q,\beta) \cong 2e^{-3i\pi/4-ik(p+q)} \int_{-\infty}^{\infty} e^{-c_2s^2}ds - 2e^{-3i\pi/4-ik(p+q)}c_4 \int_{-\infty}^{\infty} s^4e^{-(c_2-c_6/c_4)s^2}ds. \tag{69}$$

Such integrals can be evaluated by using identities given in [2]:

$$\begin{aligned} &\int_{-\infty}^{\infty} e^{-\kappa x^2}dx = \tfrac{\sqrt{\pi}}{\sqrt{\kappa}} \\ &\int_{-\infty}^{\infty} x^4e^{-\kappa x^2}dx = \tfrac{\partial^2}{\partial\kappa^2}\left\{\int_{-\infty}^{\infty} e^{-\kappa x^2}dx\right\} = \tfrac{\partial^2}{\partial\kappa^2}\left\{\tfrac{\sqrt{\pi}}{\sqrt{\kappa}}\right\} = \tfrac{3}{4}\tfrac{\sqrt{\pi}}{\kappa^{2.5}} \end{aligned} \quad , \tag{70}$$

provided $\mathrm{Re}\{\kappa\} > 0$. The answers are found to be

$$\begin{aligned} J(p,q,\beta) &\cong \frac{2e^{-3i\pi/4-ik(p+q)}\sqrt{\pi}}{\sqrt{c_2}} - \frac{2e^{-3i\pi/4-ik(p+q)}c_4\frac{3}{4}\sqrt{\pi}}{(c_2-c_6/c_4)^{2.5}} \\ &= 2e^{-3i\pi/4-ik(p+q)}\sqrt{\pi}\left[\frac{1}{\sqrt{c_2}} - \frac{\frac{3}{4}c_4}{(c_2-c_6/c_4)^{2.5}}\right]. \end{aligned} \tag{71}$$

Finally, by substituting Eqs. (71), (60), and (59) into Eq. (30), we get:

$$\begin{aligned} g(a,b,\beta) \cong\ & \tfrac{1}{2}H_0^{(2)}\left(k\sqrt{a^2+b^2-2ab\cos\beta}\right) \\ & + \tfrac{1}{2}H_0^{(2)}\left(k\sqrt{a^2+b^2-2ab\cos\beta}\right) sgn\left(\cos\tfrac{\beta}{2}\right) - \frac{sgn\left(\cos\frac{\beta}{2}\right)e^{-ik(p+q)}}{\pi\sqrt{2k(p+q)}}\left[\frac{1}{\sqrt{c_2}} - \frac{\frac{3}{4}c_4}{(c_2-c_6/c_4)^{2.5}}\right], \end{aligned} \tag{72}$$

or, using an identity $sgn(t) = 2u(t) - 1$, we can write:

$$\begin{aligned} g(a,b,\beta) \cong\ & H_0^{(2)}\left(k\sqrt{a^2+b^2-2ab\cos\beta}\right) u\left(\cos\tfrac{\beta}{2}\right) \\ & - \frac{sgn\left(\cos\frac{\beta}{2}\right)e^{-ik(p+q)}}{\pi\sqrt{2k(p+q)}}\left[\frac{1}{\sqrt{c_2}} - \frac{\frac{3}{4}c_4}{(c_2-c_6/c_4)^{2.5}}\right]. \end{aligned} \tag{73}$$

This will be convenient for numerical computations whenever Eq. (53) is not rapidly convergent. The accuracies of Eqs. (53) and (73) for various cases are compared in the next section.

4. Numerical results

Numerical results were obtained for a half plane problem in the case of a perfect electric conductor existing on the $\phi = 0^\circ$ plane as shown in Figure 1. When the source was an electric current, we used Green's function in Eq. (4) for calculating the electric fields from Eq. (5); when the source was a magnetic current we used Green's function in Eq. (1) for calculating the magnetic fields from Eq. (6). The exact solutions, E_z^{exact} or H_z^{exact}, were obtained by summing up the terms of the original series given for $g(a, b, \beta)$ in Eq. (2) until the magnitudes of the new terms relative to the total sum became less than 10^{-15}. The exact results were compared with our approximate calculations, wherein $g(a, b, \beta)$ was calculated by using only 5 terms in Eq. (53) whenever $kp \leq 2$, or using Eq. (73) whenever $kp > 2$. We also implemented the schemes of GTD and UTD for obtaining $g(a, b, \beta)$ via Eq. (7) and the approximations given in Section 2; the corresponding fields were calculated for comparison. The accuracies of the fields were compared as relative errors with respect to the exact solution, which can be expressed as

$$\varepsilon_r = \left| E_z - E_z^{exact} \right| / \left| E_z^{exact} \right| \tag{74}$$

or

$$\varepsilon_r = \left| H_z - H_z^{exact} \right| / \left| H_z^{exact} \right|. \tag{75}$$

When the parameters of the conducting half plane problem (shown in Figure 1) were $k = 1rad/m$, $a = 50m, b = 60m$, and $\phi' = 30^\circ$ and the fields were observed at $0 \leq \phi \leq 360^\circ$ for an electric current filament $I_e = 1A$, the electric fields were found as shown in Figure 6. Our results and those of the UTD overlapped with the exact solution, whereas those of the GTD diverged close to the RSB at $\phi = 150^\circ$ and $\phi = 210^\circ$ as expected. The accuracies of the three results were compared, as shown in Figure 7; our results were fairly accurate when compared with the results of the GTD and UTD.

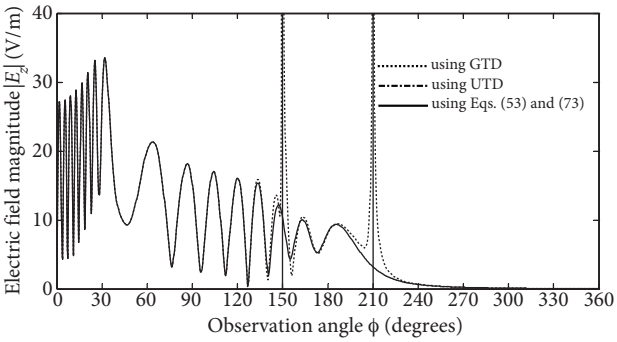

Figure 6. The electric field magnitudes for a line source $I_e = 1A$, $k = 1rad/m$, $a = 50m$, $b = 60m$, and $\phi' = 30^\circ$ versus the angle ϕ.

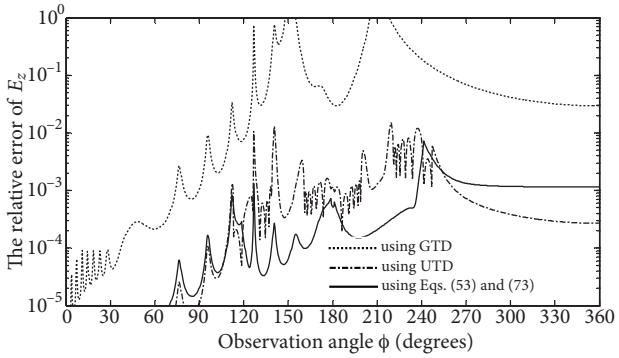

Figure 7. The relative errors of electric fields in the case mentioned in the previous figure versus the angle ϕ.

We also considered the case of the source in the problem mentioned above being a magnetic current filament $I_m = 1V$. Then the boundary conditions were of the hard polarization type. Correspondingly, the magnetic fields for parameters $k = 1rad/m$, $a = 50m$, $b = 60m$, $\phi' = 30^\circ$, and $0 \leq \phi \leq 360^\circ$ were calculated as shown in Figure 8. Again, we see that our results and those of the UTD are indistinguishable from the exact solution. However, the fields of the GTD become inaccurate near the RSB at $\phi = 150^\circ$ and $\phi = 210^\circ$, as was the case in the previously considered problem. The accuracies of the results were compared as shown in Figure 9. We can conclude from Figure 9 and also from Figure 7 that the fields calculated from the scheme in

this paper are as accurate as the fields calculated from the scheme of the UTD, whose implementation involves calculations of the Fresnel integrals.

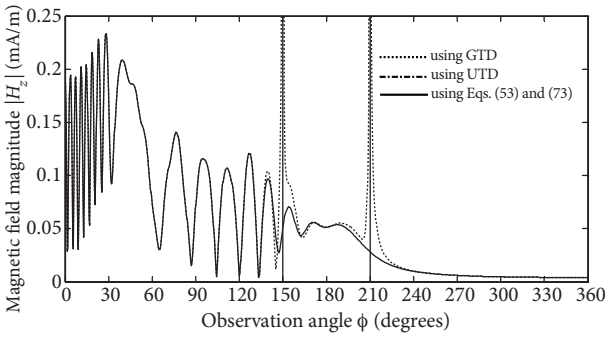

Figure 8. The magnetic field magnitudes for a line source $I_m = 1V$, $k = 1rad/m$, $a = 50m$, $b = 60m$, and $\phi' = 30°$ versus the angle ϕ.

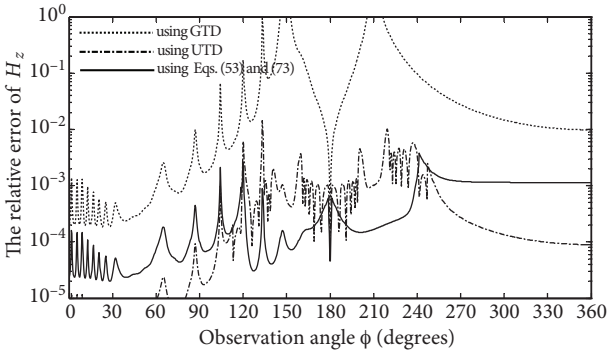

Figure 9. The relative errors of magnetic fields in the case mentioned in the previous figure versus the angle ϕ.

In the next example, we consider a case of the field observation point being too close to the edge, i.e. when ka is too small. The parameters of the conducting half plane problem were chosen to be $k = 1rad/m$, $a = 0.5m$, $b = 60m$, and $\phi' = 30°$ and the fields were observed at $0 \leq \phi \leq 360°$ for an electric current filament $I_e = 1A$. The corresponding electric fields were calculated as shown in Figure 10. We see that the curves of our results and those of the UTD almost overlap with the curve of the exact results, but those of the GTD diverge completely. A comparison between the accuracies of results was made as shown in Figure 11. The figure shows that our results are much more accurate than the results of the UTD. Namely, a relative error of 10^{-6} is numerically equivalent to 6 significant digits of accuracy, and therefore our results are very accurate.

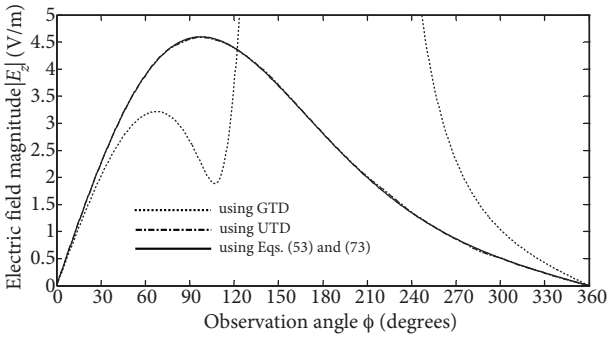

Figure 10. The electric field magnitudes for a line source $I_e = 1A$, $k = 1rad/m$, $a = 0.5m$, $b = 60m$, and $\phi' = 30°$ versus the angle ϕ.

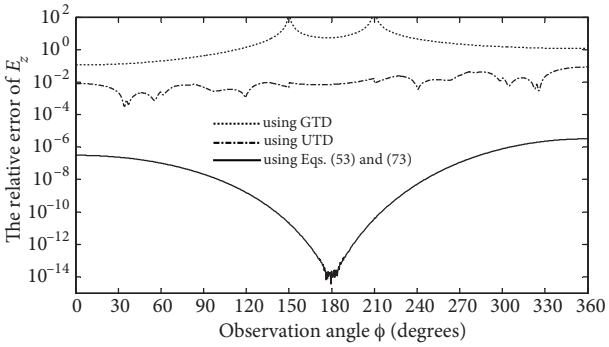

Figure 11. The relative errors of electric fields in the case mentioned in the previous figure versus the angle ϕ.

Finally, we calculated the fields in the case of the current source in the preceding problem being a magnetic current filament, while the other parameters were the same at $k = 1rad/m$, $a = 0.5m$, $b = 60m$, and $\phi' = 30°$, and the fields were observed at $0 \leq \phi \leq 360°$ for a magnetic current filament $I_m = 1V$. The magnetic fields were obtained as shown in Figure 12. We see again that our results and those of the UTD overlap, but those of the GTD are completely inaccurate. The relative errors of the fields for this case of the problem are given in Figure 13. We see that our numerical results in the worst case are accurate up to 6 significant digits.

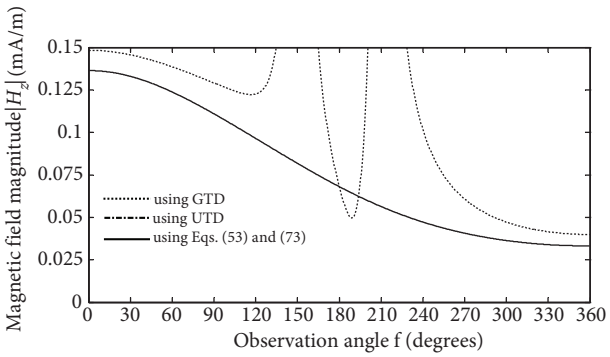

Figure 12. The magnetic field magnitudes for a line source $I_m = 1V$, $k = 1rad/m$, $a = 0.5m$, $b = 60m$, and $\phi' = 30^\circ$ versus the angle ϕ.

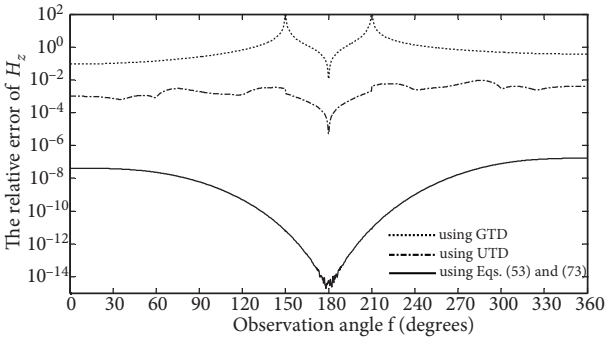

Figure 13. The relative errors of magnetic fields in the case mentioned in the previous figure versus the angle ϕ.

5. Conclusion

The asymptotic techniques in the literature such as the GTD and UTD have a limitation that the wavenumber k must be large or, equivalently, the frequency must be high. The calculations of the fields near the RSB also have some computational complexities as mentioned previously. We started from the modal solution of the problem and after some transformations, but without making any approximation, we developed a rapidly convergent series (Eq. (53)) that may be used in calculating the fields near the RSB even in the low frequency case. The terms of the series are seen to be expressible in terms of the elementary functions such as sine, cosine, and exponential functions, and therefore the summation process can be implemented easily on any computational environment.

The only limitation regarding the rapid convergence of the series in Eq. (53) is that the observation angle must be close to the RSB. For a case of the observation angle being away from the RSB, one can use the very simple expression in Eq. (73). The numerical results have shown that Eqs. (53) and (73) together yield very accurate results for electric or magnetic fields when compared with those obtainable by the schemes of GTD and UTD.

The ideas related to contour deformations when deriving Eq. (53) may be extended to other canonical problems such as diffraction by a conducting wedge or scattering by a conducting cylinder. We also demonstrated a practical application of the multiplicative calculus in the steepest descent method. When deriving Eq. (73), we evaluate an integral approximately by expanding the integrand into a Taylor "product" expansion in the sense of the multiplicative calculus. We assume that the usage of Taylor product approximations in the steepest descent method is novel since we could not detect a similar technique in the literature. The multiplicative calculus may be advantageous in many cases in electromagnetics. It may be used to improve several high frequency methods or asymptotic techniques that employ any one of the steepest descent or stationary phase methods.

References

[1] Sommerfeld A. Mathematische Theorie der Diffraktion. Mathematische Annalen 1896; 47: 314–374 (in German).

[2] Abramowitz M, Stegun I. Handbook of Mathematical Functions: With Formulas, Graphs, and Mathematical Tables. New York, NY, USA: Dover, 1970.

[3] Macdonald HM. Electric Waves. Cambridge, UK: Cambridge University Press, 1902.

[4] Keller J. Geometrical theory of diffraction. J Opt Soc Am 1962; 52: 116–130.

[5] Pathak PH, Kouyoumjian RG. The dyadic diffraction coefficient for a perfectly conducting wedge. ElectroScience Lab. Columbus, OH, USA: Ohio State University Report 2183-4, 1970.

[6] Kouyoumjian RG, Pathak PH. A uniform geometrical theory of diffraction for an edge in a perfectly conducting surface. P IEEE 1974; 62: 1448–1461.

[7] Uzer A. Multiplicative type complex calculus as an alternative to the classical calculus. Comput Math Appl 2010; 60: 2725–2737.

[8] Erdelyi A. Asymptotic Expansions. New York, NY, USA: Dover, 1956.

[9] Balanis CA. Advanced Engineering Electromagnetics. New York, NY, USA: John Wiley & Sons, 1989.